Supplemental Methods

Expression and purification of recombinant CII peptides. DNA constructs were transformed into *E. coli* BL21(DE3). 5 mL of Luria–Bertani broth (with 50 μg/mL kanamycin) was inoculated with a single colony and incubated at 37 °C with 220 rpm until an OD600 of 0.4. 1mM of isopropyl β-D-1-thiogalactopyranoside (IPTG) was added to induce expression; then the cells were incubated overnight at 22 °C with 220 rpm for 16 h. The cells were harvested by centrifugation at 3000 g for 20 min at 4°C, and were lysed in 300 μL Bugbuster (Novagen) containing protease inhibitor tablets (Roche) and benzonase (Novagen). The lysates were stored at -80°C until use. For purification, the bacteria cell pellet was lysed and the resulting supernatants containing the all CII-foldon fragments were purified by immobilized metal ion affinity chromatography using Dynabeads following the supplier's instructions (Invitrogen, Life Technologies, USA).

Surface Plasmon Resonance (SPR) determination. Binding of all synthetic triple-helical peptides to ACC1 was analyzed as previously described (1) by SPR using a Biacore T200 biosensor (GE Healthcare) at 25°C. Briefly, an anti-mouse IgG antibody was covalently coupled to a CM5 sensor chip by amino coupling. ACC1 was diluted in PBS-P running buffer (20mM phosphate buffer, 2.7 mM KCl, 137 mM NaCl and 0.05 % Surfactant P20) and injected at 10μL/min with a final concentration of 10μg/mL, to achieve a capture level of about 1000 RU. Triple-helical peptides were then injected over the sensor chip surface at a concentration of 10 μg/mL for 60 s at a flow rate of 30 μL/min, followed by a 200s dissociation phase. Before each run, all molecules previously bound on the chip (ACC1 and bound peptides) were removed by injection of regeneration solution (glycine-HCl pH 1.7). The thermodynamic (K_D) and kinetic parameters (k_{on} and k_{off}) of ACC1 binding to the selected peptides were determined by single-cycle kinetics. The assay was performed in a continuous flow of 5 μL/min in PBS-P buffer using five different concentrations of peptide (600 nM, 200 nM, 66 nM, 22 nM and 7 nM). Sensograms were processed using an automatic correction for nonspecific bulk-refractive-index effects. Data processing and analysis were performed using Biacore T200 evaluation software in a heterogenous binding model (GE Healthcare).

Enzyme-linked immunosorbent assay (ELISA). ELISA assays were performed to analyze the interaction between ACC1 and different collagens (I, II, IX and XI), Corning Costar plates (Thermo Fisher Scientific) were coated for 2 h with 5 µg/mL denatured collagen (70 °C, 30 min) and blocked with 3% heat-inactivated FBS in DPBS for 2 h at room temperature. Specific binding was detected using HRP-conjugated anti-mouse immunoglobulin kappa light chain antibody (clone 187.1; Southern Biotech) and ABTS (Roche) as substrate. Absorbance at 405 nm was measured by Synergy-2 (BioTek Instruments). An internal standard was used in all ELISA plates to allow comparison between different plates. For analysis of binding of ACC1 to CCP-1 and control peptides, streptavidin-coated high capacity plates (ThermoFisher Scientific) were used to capture the biotinylated peptides for 2 h at RT followed by detection as described above. The Immunoscan CCPlus® Kit (Euro Diagnostica) was used to analyze the binding of mouse monoclonal antibodies ACC1, ACC3, ACC4 and a monoclonal antibody 15A specific for cartilage oligomeric matrix protein (2). Most of the procedures were performed in accordance with the manufacturer's instructions, with the exception that HRP-conjugated anti-mouse immunoglobulin kappa light chain antibody (clone 187.1, Southern Biotech) was used instead of the anti-human antibodies of the kits. The response was measured as described above.

Histology. Sections of about 5 µm were stained with hematoxylin/eosin or toluidine blue. For determination of mAb reactivity with joint tissue *in vivo*, 2-days old neonate Cia9i mouse were intraperitoneally injected with 100 µg of biotinylated mAbs. After 48 hours, the knee joints were snap frozen in isopentane on dry ice and stored at -80°C. Joint sections (5 µm) were fixed in 4% paraformaldehyde for 5 min, rinsed in PBS, blocked for endogenous peroxidase for 30 min (0.5% H_2O with 0.1% Tween 20), incubated with Extravidin® peroxidase (Sigma-Aldrich, Saint Louis, MO, USA) for 30 min, and developed with diaminobenzidine (DAB Kit; Dako, Copenhagen, Denmark) for 8-9 min. To assess direct binding of mAb to the tissue sections *in vitro*, limbs from 2 days old naïve Cia9i neonates were harvested and snap frozen, and cryo-sectioned. Sections of 5 µm were subjected to 5 µg/mL biotinylated mAb for 40 minutes. Extravidin® peroxidase and DAB were used for detection.

Preparation and purification of the mAb ACC1Fab fragment. mAb ACC1 hybridoma cells were cultured using CELLine 1000 flasks (Integra Biosciences). GammaBind Plus Gel Matrix (Pharmacia)

and an ÄKTA chromatography system (GE Healthcare) were used to purify the antibody from the culture supernatant. $ACC1_{Fab}$ was prepared using the ImmunoPure Fab Preparation Kit (Pierce) in accordance with the manufacturer's instructions. Papain cleavage was evaluated by sodium dodecyl sulfate (SDS) polyacrylamide gel electrophoresis. The Fab fragments used for crystallization were further purified by size exclusion chromatography with HiLoad 16/600 Superdex 200. Aliquots of purified $ACC1_{Fab}$ fragments in 20 mM Tris pH 7.4, and 50 mM NaCl were mixed with the cognate peptides (Supplementary Table 3) in 2-3 times molar excess and incubated overnight before setup of crystallization screens or storage at -80°C before further use.

Crystallization of ACC1-peptide complexes. The crystals used for data collection were grown and cryo-protected as follows:

ACC1+ C1-CIT365-L: The 2 µl hanging drop consisting of equal volumes of 10 mg/mL complex and 1 mg/mL peptide in 20 mM Tris pH 7.4, 50 mM NaCl, and reservoir solution (16% (w/v) PEG 8000, 0.1 M Hepes pH 7.0) was equilibrated against a 1 mL reservoir. The crystal was cryo-protected by brief soaking in 12% (w/v) PEG 8000, 75 mM Hepes pH 7.0, 25% (w/v) ethylene glycol.

ACC1+ C1-CIT365-T: The sitting drop was pipetted from 0.2 µl protein solution (10 mg/mL in 20 mM Tris pH 7.4, 50 mM NaCl) and 0.1 µl reservoir solution (20% (w/v) PEG 3350, 0.1 M Bistris-Propane pH 6.5, 0.2 M NaBr). The crystal was cryo-protected by brief soaking in 17% (w/v) PEG 3350, 85 mM Bistris-Propane pH 6.5, 0.17 M NaBr, 15% (w/v) ethylene glycol.

ACC1+ CII583-591($P2_12_12_1$): The 1.5 µl hanging drop consisting of 1 µl of protein solution (9 mg/mL in 20 mM Tris pH 7.4, 50 mM NaCl) and 0.5 µl reservoir solution (20% (w/v) PEG3350, 0.1 M Bistris-Propane pH 7.0, 0.2 M sodium acetate) was equilibrated against a 1 mL reservoir. The cryo-protection solution contained 15% (w/v) PEG3350, 75 mM Bistris-Propane pH 7.0, 0.15 M sodium acetate, and 25% (w/v) ethylene glycol.

ACC1+ CII583-591(P1): The sitting drop was pipetted from 0.2 µl protein solution (10 mg/mL in 20 mM Tris pH 7.4, 50 mM NaCl) and 0.1 µl reservoir solution (20% (w/v) PEG3350, 0.1 M Bistris-Propane pH 7.5, 0.2 M sodium acetate). The harvested crystal was cryo-protected by soaking in 15%

(w/v) PEG3350, 75 mM Bistris-Propane pH 7.5, 0.15 M sodium acetate, 25% (w/v) ethylene glycol.

ACC1+ CII616-639-CIT: The sitting drop consisted of 0.2 µl protein solution (10 mg/mL in 20 mM Tris pH 7.4, 50 mM NaCl) and 0.1 µl reservoir solution (20% (w/v) PEG 6000, 0.1 M MES pH 6.0, 0.2 M CaCl2). The harvested crystal was cryo-protected using 15% (w/v) PEG 6000, 75 mM MES pH 6.0, 0.15 M CaCl2, 25% (w/v) glycerol.

1. Raposo B, Dobritzsch D, Ge C, Ekman D, Xu B, Lindh I, et al. Epitope-specific antibody response is controlled by immunoglobulin V(H) polymorphisms. *J Exp Med.* 2014;211(3):405-11.
2. Geng H, Nandakumar KS, Pramhed A, Aspberg A, Mattsson R, and Holmdahl R. Cartilage oligomeric matrix protein specific antibodies are pathogenic. *Arthritis Res Ther.* 2012;14(4):R191.

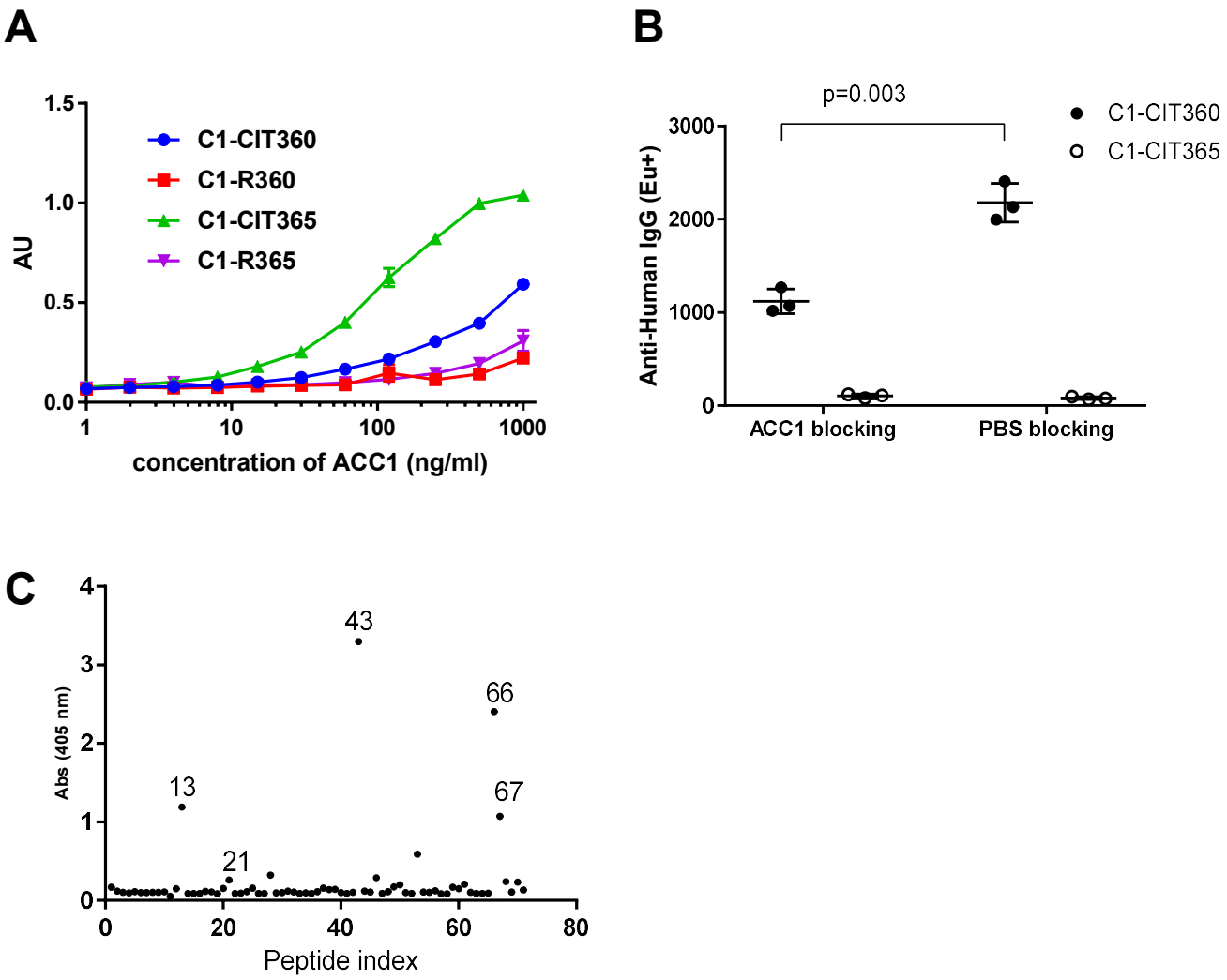

Supplementary Figure 1. Characterization of ACC1. (A). Binding of ACC1 for cyclic C1-CIT360, C1-CIT365, C1-R360 and C1-R365 were measured by ELISA. (B). Solid-phase inhibition assay. The ELISA plate coated by cyclic peptide C1-CIT360 or C1-CIT365, was pre-incubated with ACC1 (2ug/ml) and then the sera (1:300 dilution) of a pool of 6 RA patients selected for positivity against C1-CIT360 was added for 3 hours of incubation at RT. The binding of human polyclonal antibodies to the given peptides was measured. One representative experiment was shown from three assays performed using triplicate technical replicates. Data represent mean + SD and the p value was calculated by Mann-Whitney U test to compare different groups. (C). Screening of a recombinant triple-helical peptide library of collagen II with ACC1. A set of 70 recombinant triple-helical peptides was used to assess the specificity of ACC1 in ELISA. The positive peptides are indicated. 13, CII121-144; 21, CII241-264; 43, CII571-591; 66, CII916-939; 67, CII931-954.

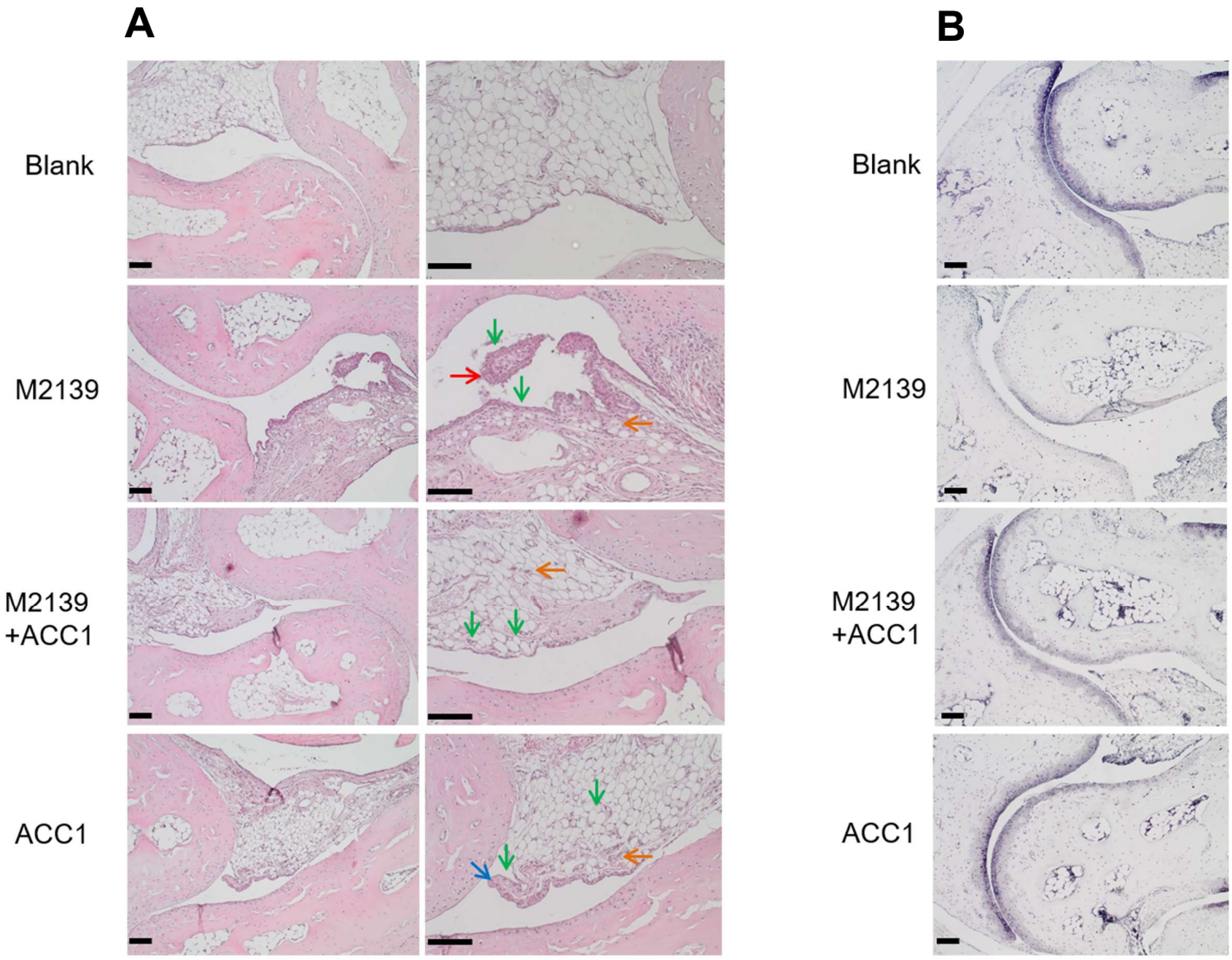

Supplementary Figure 2. Histology of tarsal joint sections. Paws of B10Q mice on day 12 after the antibody transfer were collected, fixed, decalcified, sectioned and stained with hematoxylin/eosin (A) or toluidine blue (b). (a) From top to bottom panel, mice were injected with PBS, M2139, M2139+ACC1, and ACC1, respectively. Hyperplasia is marked by red arrow, and infiltration is marked by orange arrow, while angiogenesis and pannus formation are indicated by a green and blue arrow, respectively. (B) From top to bottom panel, mice were injected with PBS, M2139, M2139+ACC1, ACC1, respectively, and stained with toluidine blue to visualize proteoglycan levels. Loss of proteoglycan staining was observed in the M2139, M2139+ACC1, ACC1 groups. Results shown are representative of those obtained from 6 mice in each group. The scale bar represents 100 μm.

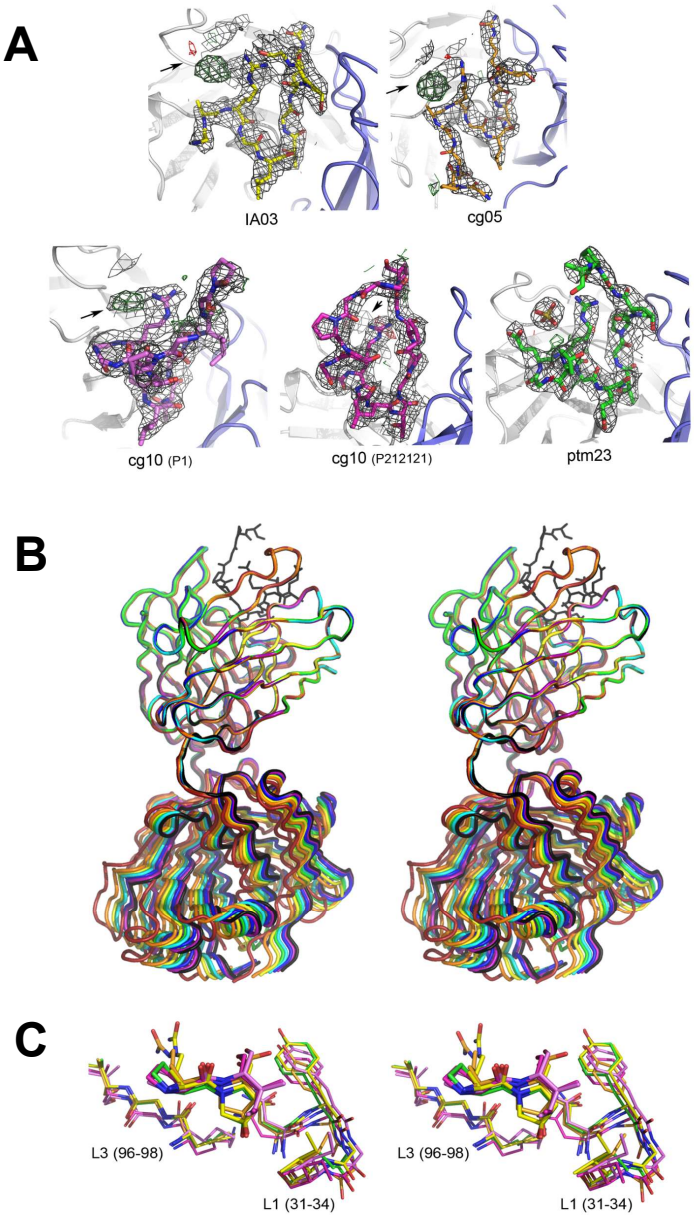

Supplementary Figure 3. Structural analysis of the ACC1$_{Fab}$-peptide complexes. (A). The electron density observed for the peptides bound to ACC1. The final $2F_o$-F_c electron density map contoured at 1 σ is shown in grey, whereas peaks in the F_o-F_c map contoured at 3 and -3 σ are shown in green and red, respectively. The density observed for the unidentified ion is marked by an arrow. The heavy and light chains of the ACC1$_{Fab}$ are depicted in cartoon representation in white and blue, respectively. The bound peptides are shown as sticks with carbon atoms in yellow (C1-CIT365-L), orange (C1-CIT365-T), mauve (CII538-591 in space group P1), magenta (CII538-591 in space group $P2_12_12_1$), and green (CII616-639-CIT), respectively. (B). The VH-domain based superimposition of the eight complex copies present in the asymmetric unit of the ACC1$_{Fab}$-CII616-639-CIT crystal highlights the variation in their elbow angles. Each complex copy is colored differently. For clarity, only one copy of the bound CII616-639-CIT peptide is shown (black sticks). The relative orientation between the variable and constant Fab domains is significantly influenced by crystal packing as indicated by the wide spread of elbow angles calculated for the eight Fab copies per asymmetric unit (e.g. 135-147° for the ACC1Fab-CII616-639-CIT complex). (C). Stereo view of the superposed stretches of the L1 and L3 loops of all ACC1$_{Fab}$-peptide complexes that show larger structural deviation due to a sequence variation upstream of the conserved motif in the bound peptides, with Cit-Hyp in C1-CIT365-T and C1-CIT365-L corresponding to Pro-Ile in CII583-591 and Pro-Hyp in CII616-639. For clarity, only these two residues of the peptide are shown (thicker sticks). Carbon atom colors of bound peptide as well as the L1 and L3 residues of the distinct complexes correspond to those used in (A).

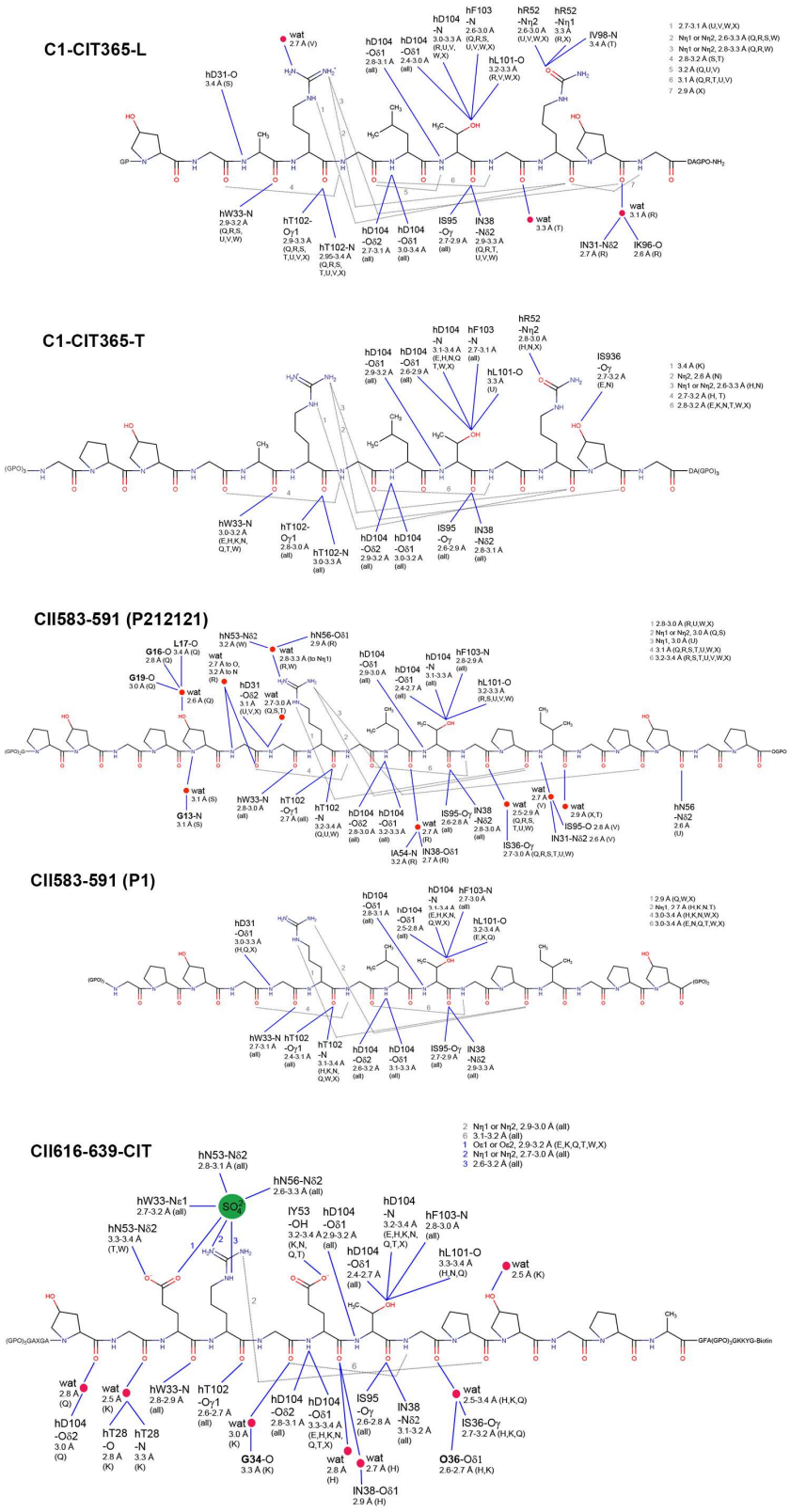

Supplementary Figure 4. Schematic presentation of peptide binding site in ACC1Fab. The key residues from both heavy chain and light chain of ACC1Fab participating in the hydrogen bonds with the peptide are shown. Hydrogen bonds are illustrated as black lines. Carbon atoms are colored in black, nitrogen atoms in blue, and oxygen atoms in red. For the numbered intrapeptide hydrogen bonds, this information is provided in the legend within the figure. A counter ion found in nearly all structures but only was colored green in $ACC1_{Fab}$-CII616-639. For $ACC1_{Fab}$ residues, the heavy or light chain origin is indicated by an h or l suffix, respectively, followed by the residue type and number, and the name of the atom forming the hydrogen bond.

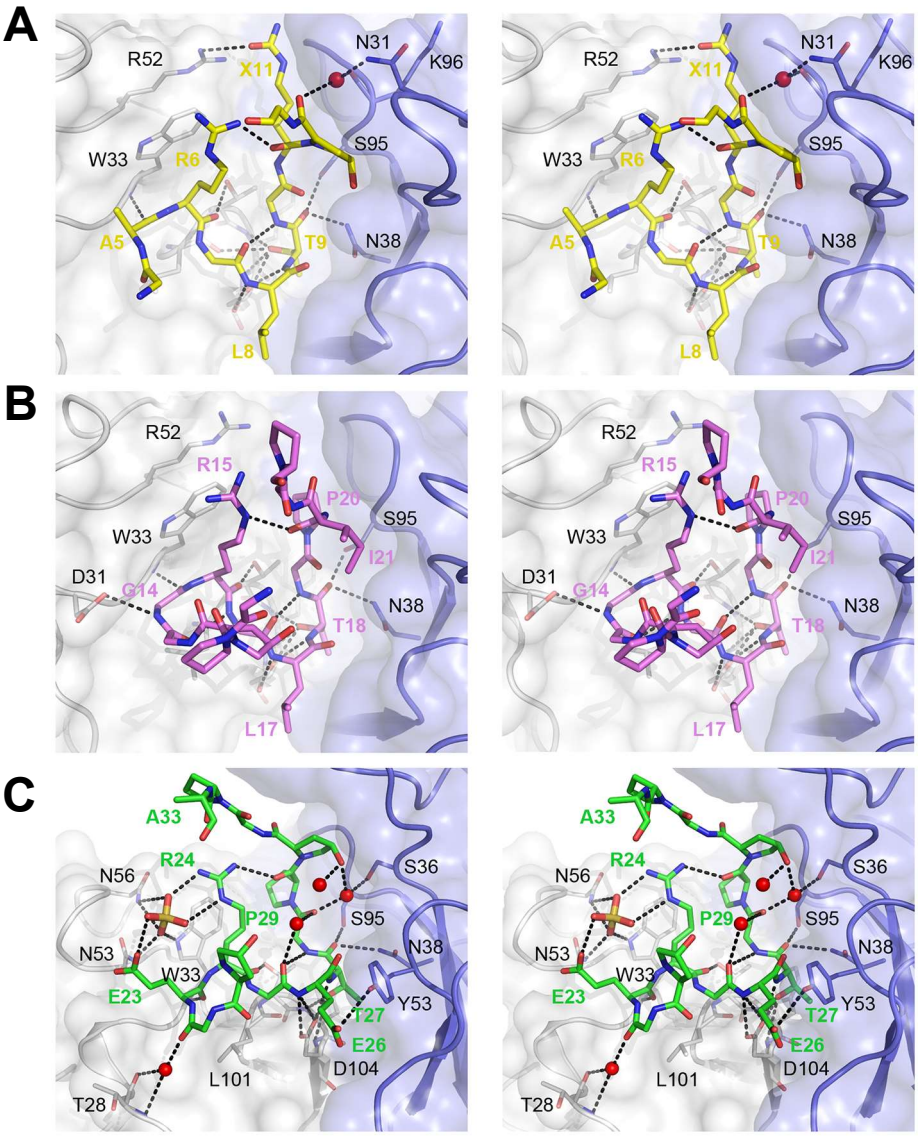

Supplementary Figure 5. Hydrogen bonding network formed upon peptide binding to acc1, with emphasis on non-conserved interactions. The chosen orientation focuses on less or non-conserved hydrogen bond interactions of peptide residues surrounding the conserved RG-TG motif. The heavy and light chains of the $ACC1_{Fab}$ are shown as cartoon in white and blue, respectively, and the dimensions of the paratope outlined by the semitransparent molecular envelop. ACC1 residues forming hydrogen bonds to the peptide are shown as sticks, with carbon atoms colored black. Hydrogen bonds are indicated as black dotted lines, water molecules as red spheres. The peptides are shown as thicker sticks, with carbon atoms in yellow (C1-CIT365-L), mauve (CII538-591 in space group P1), and green (CII616-639-CIT), respectively. All peptide residues other than glycine, proline (except the proline occurring in CII538-591 and CII616-639-CIT at the same position as the citrulline in C1-CIT365-L and C1-CIT365-T), and 4-hydroxyproline are labeled in bold and according color. (A) $ACC1_{Fab}$-C1-CIT365-L, (B) $ACC1_{Fab}$-CII538-591 as in P1 space group, (C) $ACC1_{Fab}$-CII616-639-CIT.

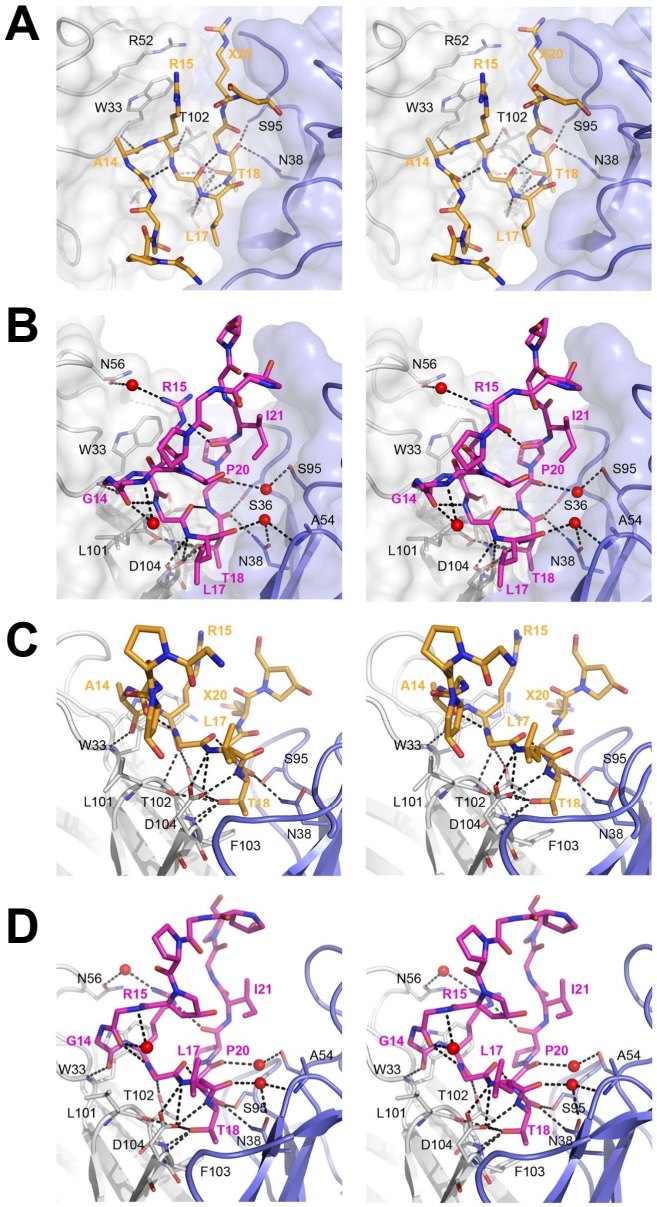

Supplementary Figure 6. Hydrogen bonding network formed upon C1-CIT365-T and CII538-591 binding to ACC1. The orientation chosen for A and B focuses on less or non-conserved hydrogen bond interactions of peptide residues surrounding the conserved RG-TG motif, that chosen for C and D on the conserved interactions between the threonine of the conserved peptide motif and the H3 CDR loop. The heavy and light chains of the $ACC1_{Fab}$ are shown as cartoon in white and blue, respectively, and the dimensions of the paratope outlined by the semitransparent molecular envelop. ACC1 residues are shown as sticks, with carbon atoms colored black. Hydrogen bonds are indicated as black dotted lines, water molecules as red spheres. The peptides are shown as thicker sticks, with carbon atoms in orange (C1-CIT365-T) and magenta (CII538-591 in space group $P2_12_12_1$), respectively. All peptide residues other than glycine, proline (except the proline occurring in CII538-591 at the same position as the citrulline in C1-CIT365-T), and 4-hydroxyproline are labeled in bold and according color. (A, C) $ACC1_{Fab}$-C1-CIT365-T, (B, D) $ACC1_{Fab}$-CII538-591 as in $P2_12_12_1$ space group.

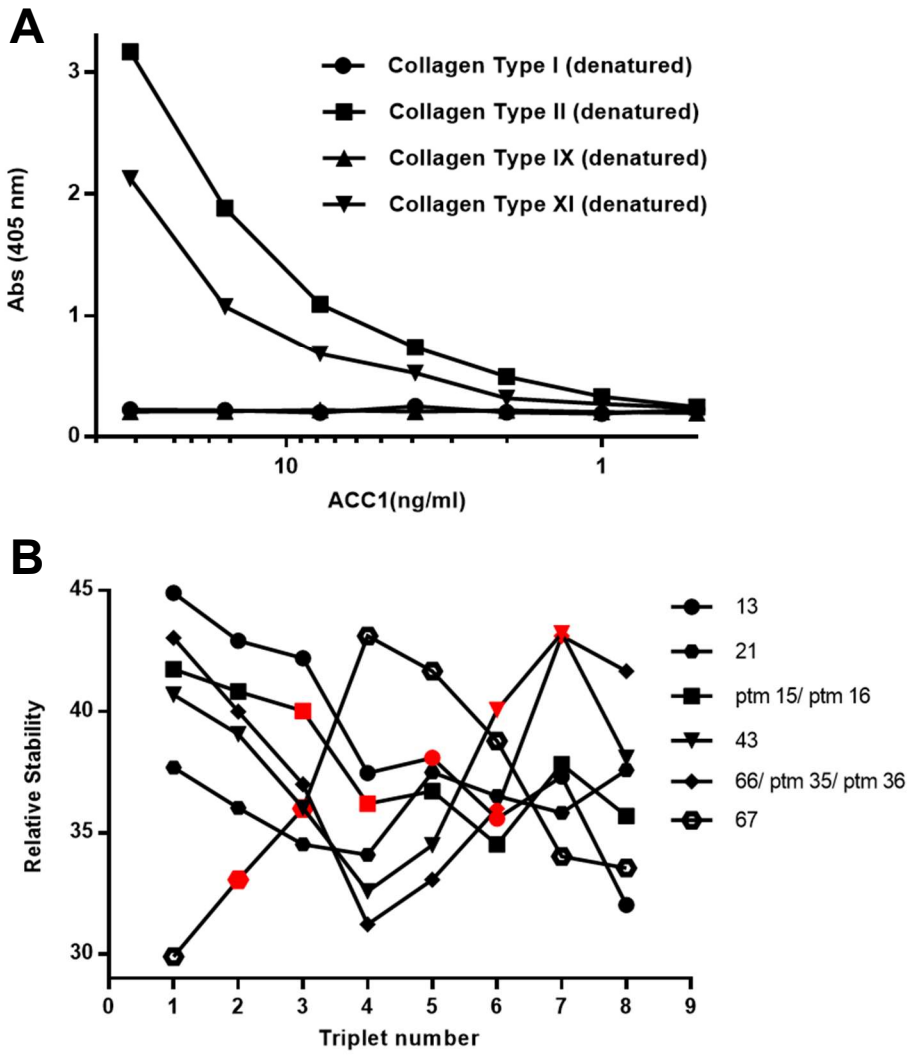

Supplementary Figure 7. Characterization of ACC1 antibody. (A) Reactivity of ACC1 towards denatured CI, CII, CIX, and CXI in ELISA. The Corning Costar plates (Thermo Fisher Scientific) were coated for 2 h with 5 µg/ml denatured collagen (70 °C, 30 min) and blocked with 3% heat-inactivated FBS in DPBS for 2 h at room temperature. Specific binding was detected using HRP-conjugated anti-mouse immunoglobulin kappa light chain antibody (clone 187.1; Southern Biotech) and ABTS (Roche) as substrate. Absorbance at 405 nm was measured with a Synergy-2 (BioTek Instruments). (B) Calculated relative stability profiles for the triple-helical peptides bound by ACC1. The binding core site covering two triplets (6 amino acids) is shown in red. 13, CII121-144; 21, CII241-264; 43, CII571-591; 66, CII916-939; 67, CII931-954; ptm15/ptm16, C1-T-CIT365; ptm35/36, F4-T-CIT933.

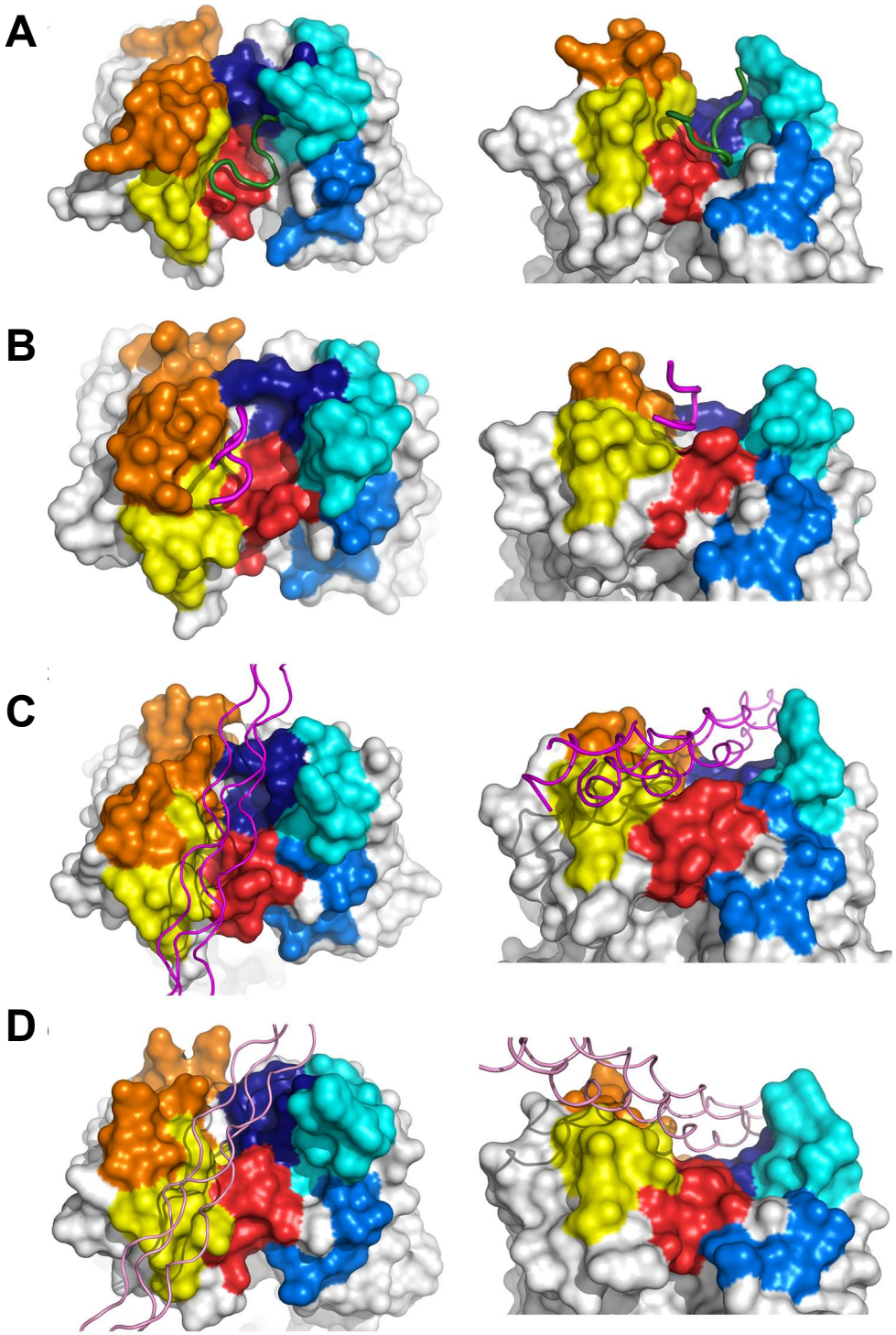

Supplementary Figure 8. Comparison of the peptide binding paratopes of ACC1, ACC4, CIIC1 and M2139. The respective Fab is shown in surface representation. The CDR loops of the heavy chain are colored yellow (H1), orange (H2) and red (H3), those of the light chain cyan (L1), marine (L2), and dark blue (L3). The cartoon representation of the C1-CIT365-L peptide bound to the $ACC1_{Fab}$ is shown in dark green (A), and that of the C1Cit1 peptide bound to the $ACC4_{Fab}$ in magenta (B). The cartoon representation of the triple-helical C1 peptide bound to the $CIIC1_{Fab}$ in shown in magenta (C) and that of the triple-helical J1 peptide bound to the $M2139_{Fab}$ in pink (D).

Supplementary Table 1. Synthetic CII peptides used in both Luminex assay (cyclic pepties) and SPR (triple-helical peptides) analysis.

All triple-helical peptides (107) were synthesized with 5 GPO repeats at both ends to facilitate the self-assembly of triple-helical strands. There is no lysine knot on these triple helical peptides. A biotin moiety is added to the N terminal GPO repeat. But for luminex assay, a new set of triple-helical peptide was synthesized as detailed in the text, and a lysine knot as shown in Figure 1A was also added. As for 54 cyclic CII peptides, two Cys residues were added to both ends and synthesized as cyclic peptide. As for the corresponding control peptides, citrulline (X) is replaced with arginine. O represents hydroxylproline; X represents citrulline.

Name	Conformation	Sequence
CII_LT_1	triple-helical(self-assembly)	GPKGPOGPQGPAGEQGPRGDRGDK
CII_LT_2	triple-helical(self-assembly)	GPRGDRGDKGEKGAOGPRGRDGEO
CII_LT_3	triple-helical(self-assembly)	GPRGRDGEOGTOGNOGPO
CII_LT_4	triple-helical(self-assembly)	GLGGNFAAQMAGGFDEKAGGAQLGVMQ
CII_LT_5	triple-helical(self-assembly)	GPMGPMGPRGPOGPAGAOGPQGFQ
CII_LT_6	triple-helical(self-assembly)	GAOGPQGFQGNOGEOGEOGVSGPM
CII_LT_7	triple-helical(self-assembly)	GEOGVSGPMGPRGPOGPOGKOGDD
CII_LT_8	triple-helical(self-assembly)	GKOGDDGEAGKOGKAGERGPO
CII_LT_9	triple-helical(self-assembly)	GKAGERGPOGPQGARGFOGTOGLO
CII_LT_10	triple-helical(self-assembly)	GFOGTOGLOGVKGHRGYOGLDGAK
CII_LT_11	triple-helical(self-assembly)	GYOGLDGAKGEAGAOGVKGESGSO
CII_LT_12	triple-helical(self-assembly)	GVKGESGSOGENGSOGPMGPRGLO
CII_LT_E41_R-R-R	triple-helical(self-assembly)	GPMGPRGLOGERGRTGPAGAAGAR
CII_LT_14	triple-helical(self-assembly)	GPAGAAGARGNDGQOGPAGPOGPV
CII_LT_15	triple-helical(self-assembly)	GPAGPOGPVGPAGGOGFOGAOGAK
CII_LT_(TD1)_R-(R)	triple-helical(self-assembly)	GFOGAOGAKGEAGPTGARGPEGAQ
CII_LT_TD1_R-R	triple-helical(self-assembly)	GARGPEGAQGPRGEOGTOGSOGPA

CII_LT_E17	triple-helical(self-assembly)	GTOGSOGPAGASGNOGTDGIOGAK
CII_LT_19	triple-helical(self-assembly)	GTDGIOGAKGSAGAOGIAGAOGFO
CII_LT_20	triple-helical(self-assembly)	GIAGAOGFOGPRGPOGPQGATGPL
CII_LT_21	triple-helical(self-assembly)	GPQGATGPLGPKGQTGEOGIAGFK
CII_LT_T	triple-helical(self-assembly)	GEOGIAGFKGEQGPKGEOGPAGPQ
CII_LT_23	triple-helical(self-assembly)	GEOGPAGPQGAOGPAGEEGKRGAR
CII_LT_24	triple-helical(self-assembly)	GEEGKRGARGEOGGVGPIGPOGER
CII_LT_25	triple-helical(self-assembly)	GPIGPOGERGAOGNRGFOGQDGLA
CII_LT_26	triple-helical(self-assembly)	GFOGQDGLAGPKGAOGERGPSGLA
CII_LT_27	triple-helical(self-assembly)	GERGPSGLAGPKGANGDOGROGEO
CII_LT_C1_R-R	triple-helical(self-assembly)	GDOGROGEOGLOGARGLTGROGDA
CII_LT_C1_R-R wP	triple-helical(self-assembly)	GDPGRPGEPGLPGARGLTGRPGDA
CII_L_C1_R-R	triple-helical(self-assembly)	GDOGROGEOGLOGARGLTGROGDA
CII_L_C1_R-R wP	triple-helical(self-assembly)	GDPGRPGEPGLPGARGLTGRPGDA
CII_LT_TD8	triple-helical(self-assembly)	GLTGROGDAGPQGKVGPSGAOGED
CII_LT_30	triple-helical(self-assembly)	GPSGAOGEDGROGPOGPQGARGQO
CII_LT_31	triple-helical(self-assembly)	GPQGARGQOGVMGFOGPKGANGEO
CII_LT_32	triple-helical(self-assembly)	GPKGANGEOGKAGEKGLOGAOGLR
CII_LT_33	triple-helical(self-assembly)	GLOGAOGLRGLOGKDGETGAAGPO
CII_LT_34	triple-helical(self-assembly)	GETGAAGPOGPAGPAGERGEQGAO
CII_LT_35	triple-helical(self-assembly)	GERGEQGAOGPSGFQGLO
CII_LT_36	triple-helical(self-assembly)	GLOGPOGPOGEGGKOGDQGVOGEA
CII_LT_U1_R-R	triple-helical(self-assembly)	GDQGVOGEAGAOGLVGPRGERGFO
CII_LT_38	triple-helical(self-assembly)	GPRGERGFOGERGSOGAQGLQGPR
CII_LT_39	triple-helical(self-assembly)	GAQGLQGPRGLOGTOGTDGPKGAS
CII_LT_40	triple-helical(self-assembly)	GTDGPKGASGPAGPOGAQGPOGLQ
CII_LT_J1_R	triple-helical(self-assembly)	GAQGPOGLQGMOGERGAAGIAGPK

CII_LT_J1_(R)	triple-helical(self-assembly)	GAAGIAGPKGDRGDVGEKGPEGAO
CII_LT_43	triple-helical(self-assembly)	GEKGPEGAOGKDGGRGLTGPIGPO
CII_LT_44	triple-helical(self-assembly)	GLTGPIGPOGPAGANGEKGEVGPO
CII_LT_45	triple-helical(self-assembly)	GEKGEVGPOGPAGSAGARGAOGER
CII_LT_46	triple-helical(self-assembly)	GARGAOGERGETGPOGPAGFAGPO
CII_LT_47	triple-helical(self-assembly)	GPAGFAGPOGADGQOGAKGEQGEA
CII_LT_48	triple-helical(self-assembly)	GAKGEQGEAGQKGDAGAOGPQGPS
CII_LT_49	triple-helical(self-assembly)	GAOGPQGPSGAOGPQGPTGVTGPK
CII_LT_D3_R	triple-helical(self-assembly)	GPTGVTGPKGARGAQGPOGATGFO
CII_LT_D3_(R)	triple-helical(self-assembly)	GPOGATGFOGAAGRVGPOGSNGNO
CII_LT_52	triple-helical(self-assembly)	GPOGSNGNOGPOGPOGPSGKDGPK
CII_LT_53	triple-helical(self-assembly)	GPSGKDGPKGARGDSGPOGRAGEO
CII_LT_54	triple-helical(self-assembly)	GPOGRAGEOGLQGPAGPOGEKGEO
CII_LT_55	triple-helical(self-assembly)	GPOGEKGEOGDDGPSGAEGPOGPQ
CII_LT_E10_R	triple-helical(self-assembly)	GAEGPOGPQGLAGQRGIVGLOGQR
CII_LT_57	triple-helical(self-assembly)	GIVGLOGQRGERGFOGLOGPSGEO
CII_LT_58	triple-helical(self-assembly)	GLOGPSGEOGKQGAOGASGDRGPO
CII_LT_59	triple-helical(self-assembly)	GASGDRGPOGPVGPOGLTGPAGEO
CII_LT_60	triple-helical(self-assembly)	GLTGPAGEOGREGSOGADGPOGRD
CII_LT_61	triple-helical(self-assembly)	GADGPOGRDGAAGVKGDRGETGAV
CII_LT_62	triple-helical(self-assembly)	GDRGETGAVGAOGAOGPOGSOGPA
CII_LT_63	triple-helical(self-assembly)	GPOGSOGPAGPTGKQGDRGEAGAQ
CII_LT_64	triple-helical(self-assembly)	GDRGEAGAQGPMGPSGPAGARGIQ
CII_LT_65	triple-helical(self-assembly)	GPAGARGIQGPQGPRGDKGEAGEO
CII_LT_F4_R-R	triple-helical(self-assembly)	GDKGEAGEOGERGLKGHRGFTGLQ
CII_L_F4_R-R	triple-helical(self-assembly)	GDKGEAGEOGERGLKGHRGFTGLQ
CII_LT_F4_R-R (no knot)	triple-helical(self-assembly)	GDKGEAGEOGERGLKGHRGFTGLQ

CII_LT_(F4)_(R)-R	triple-helical(self-assembly)	GHRGFTGLQGLOGPOGPSGDQGAS
CII_LT_68	triple-helical(self-assembly)	GPSGDQGASGPAGPSGPRGPOGPV
CII_LT_69	triple-helical(self-assembly)	GPRGPOGPVGPSGKDGANGIOGPI
CII_LT_70	triple-helical(self-assembly)	GANGIOGPIGPOGPRGRSGETGPAGPOGNO
CII_LT_1_CIT	triple-helical(self-assembly)	GKAGERGPOGPEGARGFOGTOGLO
CII_LT_E41_R-CIT-R	triple-helical(self-assembly)	GPMGPRGLOGECITGRTGPAGAAGAR
CII_LT_T_E	triple-helical(self-assembly)	GEOGIAGFKGEEGPKGEOGPAGPQ
CII_LT_T	triple-helical(self-assembly)	GEOGIAGFKGEQGPKGEOGPAGPQ
CII_LT_5_CIT	triple-helical(self-assembly)	GEEGKRGACITGEOGGVGPIGPOGER
CII_LT_6_CIT	triple-helical(self-assembly)	GFOGQDGLAGPKGAOGECITGPSGLA
CII_LT_7_CIT	triple-helical(self-assembly)	GECITGPSGLAGPKGANGDOGROGEO
CII_LT_C1_CIT-R	triple-helical(self-assembly)	GDOGROGEOGLOGACITGLTGROGDA
CII_LT_C1_CIT-CIT	triple-helical(self-assembly)	GDOGROGEOGLOGACITGLTGCITOGDA
CII_LT_C1_R-CIT	triple-helical(self-assembly)	GDOGROGEOGLOGARGLTGCITOGDA
CII_LT_C1_R-R	triple-helical(self-assembly)	GLOGARGLTGROGDAGPQGKVGPS
CII_LT_C1_CIT-R	triple-helical(self-assembly)	GLOGACITGLTGROGDAGPQGKVGPS
CII_LT_C1_CIT-CIT	triple-helical(self-assembly)	GLOGACITGLTGCITOGDAGPQGKVGPS
CII_LT_C1_CIT-CIT-E	triple-helical(self-assembly)	GLOGACITGLTGCITOGDAGPEGKVGPS
CII_LT_C1_R-CIT	triple-helical(self-assembly)	GLOGARGLTGCITOGDAGPQGKVGPS
CII_LT_C1_R-CIT-E	triple-helical(self-assembly)	GLOGARGLTGCITOGDAGPEGKVGPS

CII_LT_C1_CIT-R-E	triple-helical(self-assembly)	GLOGACITGLTGROGDAGPEGKVGPS
CII_LT_(C1)_(R)-R	triple-helical(self-assembly)	GLTGCITOGDAGPQGKVGPSGAOGED
CII_LT_(C1)_(R)-R-E	triple-helical(self-assembly)	GLTGROGDAGPEGKVGPSGAOGED
CII_LT_(C1)_(R)-CIT-E	triple-helical(self-assembly)	GLTGCITOGDAGPEGKVGPSGAOGED
CII_LT_21_CIT	triple-helical(self-assembly)	GPRGERGFOGECITGSOGAQGLQGPR
CII_LT_22_CIT	triple-helical(self-assembly)	GEKGEVGPOGPAGSAGACITGAOGER
CII_LT_23_CIT	triple-helical(self-assembly)	GACITGAOGERGETGPOGPAGFAGPO
CII_LT_D3_R-E	triple-helical(self-assembly)	GPTGVTGPKGARGAEGPOGATGFO
CII_LT_E10_CIT-Q	triple-helical(self-assembly)	GAEGPOGPQGLAGQCITGIVGLOGQR
CII_LT_E10_CIT-E	triple-helical(self-assembly)	GAEGPOGPQGLAGQCITGIVGLOGER
CII_LT_E10_R-E	triple-helical(self-assembly)	GAEGPOGPQGLAGQRGIVGLOGER
CII_LT_E10_R-Q	triple-helical(self-assembly)	GPQGLAGQRGIVGLOGQRGERGFO
CII_LT_E10_CIT-Q	triple-helical(self-assembly)	GPQGLAGQCITGIVGLOGQRGERGFO
CII_LT_E10_CIT-E	triple-helical(self-assembly)	GPQGLAGQCITGIVGLOGERGERGFO
CII_LT_E10_R-E	triple-helical(self-assembly)	GPQGLAGQRGIVGLOGERGERGFO
CII_LT_32_E	triple-helical(self-assembly)	GIVGLOGERGERGFOGLOGPSGEO
CII_LT_33_CIT	triple-helical(self-assembly)	GADGPOGCITDGAAGVKGDRGETGAV
CII_LT_34_CIT	triple-helical(self-assembly)	GPOGSOGPAGPTGKQGDCITGEAGAQ
CII_LT_F4_R-CIT	triple-helical(self-assembly)	GDKGEAGEOGERGLKGHCITGFTGLQ

CII_LT_F4_CIT-CIT	triple-helical(self-assembly)	GDKGEAGEOGECITGLKGHCITGFTGLQ
CII_LT_F4_CIT-R	triple-helical(self-assembly)	GDKGEAGEOGECITGLKGHRGFTGLQ
CII_C_1_CIT	cyclic (via disulphide bond)	Biotin-Ahx-CPMGPMGPXGPPGPAGCA
CII_C_2_CIT	cyclic (via disulphide bond)	Biotin-Ahx-CVSGPMGPXGPPGPPGCA
CII_C_3_CIT	cyclic (via disulphide bond)	Biotin-Ahx-CKPGKAGEXGPPGPQGCA
CII_C_4_CIT	cyclic (via disulphide bond)	Biotin-Ahx-CPPGPQGAXGFPGTPGCA
CII_C_5_CIT	cyclic (via disulphide bond)	Biotin-Ahx-CLPGVKGHXGYPGLDGCA
CII_C_(E41)_[CIT]-R-(R)	cyclic (via disulphide bond)	Biotin-Ahx-CSPGPMGPXGLPGERGCA
CII_C_(E41)_R-[CIT]-R	cyclic (via disulphide bond)	Biotin-Ahx-CPRGLPGEXGRTGPAGCA
CII_C_(E41)_(R)-R-[CIT]	cyclic (via disulphide bond)	Biotin-Ahx-CGLPGERGXTGPAGAACA
CII_C_9_CIT	cyclic (via disulphide bond)	Biotin-Ahx-CPAGAAGAXGNDGQPGCA
CII_C_(TD1)_[CIT]-(R)	cyclic (via disulphide bond)	Biotin-Ahx-CEAGPTGAXGPEGAQGCA
CII_C_(TD1)_(R)-[CIT]	cyclic (via disulphide bond)	Biotin-Ahx-CPEGAQGPXGEPGTPGCA
CII_C_12_CIT	cyclic (via disulphide bond)	Biotin-Ahx-CAPGFPGPXGPPGPQGCA
CII_C_13_CIT	cyclic (via disulphide bond)	Biotin-Ahx-CPAGEEGKXGARGEPGCA
CII_C_14_CIT	cyclic (via disulphide bond)	Biotin-Ahx-CEEGKRGAXGEPGGVGCA
CII_C_15_CIT	cyclic (via disulphide bond)	Biotin-Ahx-CPIGPPGEXGAPGNRGCA
CII_C_16_CIT	cyclic (via disulphide bond)	Biotin-Ahx-CERGAPGNXGFPGQDGCA
CII_C_17_CIT	cyclic (via disulphide bond)	Biotin-Ahx-CPKGAPGEXGPSGLAGCA
CII_C_18_CIT	cyclic (via disulphide bond)	Biotin-Ahx-CGANGDPGXPGEPGLPCA
CII_C_(C1)_[CIT]-R	cyclic (via disulphide bond)	Biotin-Ahx-CEPGLPGAXGLTGRPGCA
CII_C_C1_R-[CIT]	cyclic (via disulphide bond)	Biotin-Ahx-CGARGLTGXPGDAGPQCA
CII_C_21_CIT	cyclic (via disulphide bond)	Biotin-Ahx-CGAPGEDGXPGPPGPQCA
CII_C_22_CIT	cyclic (via disulphide bond)	Biotin-Ahx-CPPGPQGAXGQPGVMGCA
CII_C_23_CIT	cyclic (via disulphide bond)	Biotin-Ahx-CLPGAPGLXGLPGKDGCA

CII_C_24_CIT	cyclic (via disulphide bond)	Biotin-Ahx-CPAGPAGEXGEQGAPGCA
CII_C_U1_[CIT]-R	cyclic (via disulphide bond)	Biotin-Ahx-CAPGLVGPXGERGFPGCA
CII_C_U1_R-[CIT]	cyclic (via disulphide bond)	Biotin-Ahx-CLVGPRGEXGFPGERGCA
CII_C_27_CIT	cyclic (via disulphide bond)	Biotin-Ahx-CGRGFPGEXGSPGAQGCA
CII_C_28_CIT	cyclic (via disulphide bond)	Biotin-Ahx-CAQGLQGPXGLPGTPGCA
CII_C_(J1)_CIT	cyclic (via disulphide bond)	Biotin-Ahx-CLQGMPGEXGAAGIAGCA
CII_C_30_CIT	cyclic (via disulphide bond)	Biotin-Ahx-CIAGPKGDXGDVGEKGCA
CII_C_31_CIT	cyclic (via disulphide bond)	Biotin-Ahx-CAPGKDGGXGLTGPIGCA
CII_C_32_CIT	cyclic (via disulphide bond)	Biotin-Ahx-CPAGSAGAXGAPGERGCA
CII_C_33_CIT	cyclic (via disulphide bond)	Biotin-Ahx-CARGAPGEXGETGPPGCA
CII_C_(D3)_CIT	cyclic (via disulphide bond)	Biotin-Ahx-CVTGPKGAXGAQGPPGCA
CII_C_35_CIT	cyclic (via disulphide bond)	Biotin-Ahx-CGFPGAAGXVGPPGSNCA
CII_C_36_CIT	cyclic (via disulphide bond)	Biotin-Ahx-CKDGPKGAXGDSGPPGCA
CII_C_37_CIT	cyclic (via disulphide bond)	Biotin-Ahx-CGDSGPPGXAGEPGLQCA
CII_C_E10_CIT	cyclic (via disulphide bond)	Biotin-Ahx-CPQGLAGQXGIVGLPGCA
CII_C_39_CIT	cyclic (via disulphide bond)	Biotin-Ahx-CIVGLPGQXGERGFPGCA
CII_C_40_CIT	cyclic (via disulphide bond)	Biotin-Ahx-CLPGQRGEXGFPGLPGCA
CII_C_41_CIT	cyclic (via disulphide bond)	Biotin-Ahx-CAPGASGDXGPPGPVGCA
CII_C_42_CIT	cyclic (via disulphide bond)	Biotin-Ahx-CGPAGEPGXEGSPGADCA
CII_C_43_CIT	cyclic (via disulphide bond)	Biotin-Ahx-CGADGPPGXDGAAGVKCA
CII_C_44_CIT	cyclic (via disulphide bond)	Biotin-Ahx-CAAGVKGDXGETGAVGCA
CII_C_45_CIT	cyclic (via disulphide bond)	Biotin-Ahx-CPTGKQGDXGEAGAQGCA
CII_C_46_CIT	cyclic (via disulphide bond)	Biotin-Ahx-CPSGPAGAXGIQGPQGCA
CII_C_47_CIT	cyclic (via disulphide bond)	Biotin-Ahx-CIQGPQGPXGDKGEAGCA
CII_C_(F4)_[CIT]-R	cyclic (via disulphide bond)	Biotin-Ahx-CEAGEPGEXGLKGHRGCA
CII_C_F4_R-[CIT]	cyclic (via disulphide bond)	Biotin-Ahx-CERGLKGHXGFTGLQGCA
CII_C_50_CIT	cyclic (via disulphide bond)	Biotin-Ahx-CPAGPSGPXGPPGPVGCA

CII_C_51_CIT	cyclic (via disulphide bond)	Biotin-Ahx-CPIGPPGPXGRSGETGCA
CII_C_52_CIT	cyclic (via disulphide bond)	Biotin-Ahx-CGPPGPRGXSGETGPACA
CII_C_53_CIT	cyclic (via disulphide bond)	Biotin-Ahx-CAFAGLGPXEKGPDPLCA
CII_C_54_CIT	cyclic (via disulphide bond)	Biotin-Ahx-CPDPLQYMXADQAAGGCA

Supplementary Table 2. The binding value of peptides for ACC1, ACC3, ACC4, CIIC1 and GB8 in Luminex assay.

All the sequences of cyclic CII peptides are the same as those shown in Table S1. While a lysine knot as shown in Figure 1A was added to all the triple-helical CII peptides used in Luminex assay. X represents citrulline; O represents hydroxylproline. The likely binding motif for ACC1 is highlighted in red. MFI, median fluorescence intensity.

Peptide ID	Sequence	Structure	ACC1	ACC3	ACC4	CIIC1	GB8
CII-C-1-Cit	CPMGPMGPXGPPGPAGCA	cyclic	45.5	861	20.5	22	34
CII-C-1-R	CPMGPMGPRGPPGPAGCA	cyclic	38.5	21	18	20	36
CII-C-10-Cit	CEAGPTGAXGPEGAQGCA	cyclic	45	2208.5	15.5	17	33
CII-C-10-R	CEAGPTGARGPEGAQGCA	cyclic	39	18	18	17	29
CII-C-11-Cit	CPEGAQGPXGEPGTPGCA	cyclic	51	26	19	21	33
CII-C-11-R	CPEGAQGPRGEPGTPGCA	cyclic	51	22	21	18.5	35
CII-C-12-Cit	CAPGFPGPXGPPGPQGCA	cyclic	48	48	19	20	37
CII-C-12-R	CAPGFPGPRGPPGPQGCA	cyclic	40	18	19	18	42
CII-C-13-Cit	CPAGEEGKXGARGEPGCA	cyclic	53	24	19	18	31
CII-C-13-R	CPAGEEGKRGARGEPGCA	cyclic	46	26	21.5	22	36
CII-C-14-Cit	CEEGKRGAXGEPGGVGCA	cyclic	38	25.5	20	20	33
CII-C-14-R	CEEGKRGARGEPGGVGCA	cyclic	34	21	18	20	32
CII-C-15-Cit	CPIGPPGEXGAPGNRGCA	cyclic	36	24	20	23	309
CII-C-15-R	CPIGPPGERGAPGNRGCA	cyclic	28	15	12	15	3865
CII-C-16-Cit	CERGAPGNXGFPGQDGCA	cyclic	46.5	32	23	21	63
CII-C-16-R	CERGAPGNRGFPGQDGCA	cyclic	36	19	15	17	398
CII-C-17-Cit	CPKGAPGEXGPSGLAGCA	cyclic	43	17	16	14	55
CII-C-17-R	CPKGAPGERGPSGLAGCA	cyclic	38	17	16.5	15	1270
CII-C-18-Cit	CGANGDPGXPGEPGLPCA	cyclic	80	23	13	17	31
CII-C-18-R	CGANGDPGRPGEPGLPCA	cyclic	76	22	18	18	34
CII-C-19-Cit	CEPGLPGA**XGLTG**RPGCA	cyclic	1524	73	5422.5	19	169
CII-C-19-R	CEPGLPGA**RGLTG**RPGCA	cyclic	2857	187	20	20	2081.5
CII-C-20-Cit	CGARGLTGXPGDAGPQCA	cyclic	96	27	21	22	33
CII-C-20-R	CGARGLTGRPGDAGPQCA	cyclic	53	25	27	25	35
CII-C-21-Cit	CGAPGEDGXPGPPGPQCA	cyclic	64.5	25	17	16	37.5
CII-C-21-R	CGAPGEDGRPGPPGPQCA	cyclic	47	21	18	17	29
CII-C-22-Cit	CPPGPQGAXGQPGVMGCA	cyclic	45	2344.5	12	12	24
CII-C-22-R	CPPGPQGARGQPGVMGCA	cyclic	38	23	21	17	30.5
CII-C-23-Cit	CLPGAPGLXGLPGKDGCA	cyclic	46	23	17	17	801
CII-C-23-R	CLPGAPGLRGLPGKDGCA	cyclic	43	19	18	18	3250
CII-C-24-Cit	CPAGPAGEXGEQGAPGCA	cyclic	49	26	19	18	29
CII-C-24-R	CPAGPAGERGEQGAPGCA	cyclic	36	21.5	21	18	33
CII-C-25-Cit	CAPGLVGPXGERGFPGCA	cyclic	47	28	22	20	34
CII-C-25-R	CAPGLVGPRGERGFPGCA	cyclic	41	23	21	22	37
CII-C-26-Cit	CLVGPRGEXGFPGERGCA	cyclic	45	28	24	24	38
CII-C-26-R	CLVGPRGERGFPGERGCA	cyclic	38	22.5	20	22	42
CII-C-27-Cit	CGRGFPGEXGSPGAQGCA	cyclic	50	24.5	22.5	24	42.5

CII-C-27-R	CGRGFPGERGSPGAQGCA	cyclic	43	20	18	19	40
CII-C-28-Cit	CAQGLQGPXGLPGTPGCA	cyclic	55.5	36	21	20	41.5
CII-C-28-R	CAQGLQGPRGLPGTPGCA	cyclic	46.5	26	22	19.5	32
CII-C-29-Cit	CLQGMPGEXGAAGIAGCA	cyclic	59	18	14	13	29
CII-C-29-R	CLQGMPGERGAAGIAGCA	cyclic	53	20	15	14	184
CII-C-2-Cit	CVSGPMGPXGPPGPPGCA	cyclic	45.5	989	23	20	35
CII-C-2-R	CVSGPMGPRGPPGPPGCA	cyclic	39	26	19	23	40.5
CII-C-30-Cit	CIAGPKGDXGDVGEKGCA	cyclic	35	19	17	15	28
CII-C-30-R	CIAGPKGDRGDVGEKGCA	cyclic	33	14	13.5	13	23
CII-C-31-Cit	CAPGKDGG**XGLTG**PIGCA	cyclic	6843.5	1290	17.5	18	42.5
CII-C-31-R	CAPGKDGG**RGLTG**PIGCA	cyclic	6830	1725.5	16	15	46
CII-C-32-Cit	CPAGSAGAXGAPGERGCA	cyclic	52	81	21.5	19	351
CII-C-32-R	CPAGSAGARGAPGERGCA	cyclic	43	21	21	19	137
CII-C-33-Cit	CARGAPGE**XGETG**PPGCA	cyclic	1024.5	29	20.5	19	5223
CII-C-33-R	CARGAPGE**RGETG**PPGCA	cyclic	3531.5	152	19	17	5761
CII-C-34-Cit	CVTGPKGAXGAQGPPGCA	cyclic	37	1243	18	18	61
CII-C-34-R	CVTGPKGARGAQGPPGCA	cyclic	188	26.5	17	16.5	86
CII-C-35-Cit	CGFPGAAGXVGPPGSNCA	cyclic	52	23	16	17	31
CII-C-35-R	CGFPGAAGRVGPPGSNCA	cyclic	43	17	14	13	31
CII-C-36-Cit	CKDGPKGAXGDSGPPGCA	cyclic	129.5	1168	13	13	25.5
CII-C-36-R	CKDGPKGARGDSGPPGCA	cyclic	1130.5	37	19	17.5	32
CII-C-37-Cit	CGDSGPPGXAGEPGLQCA	cyclic	54	24	20	20	33
CII-C-37-R	CGDSGPPGRAGEPGLQCA	cyclic	46	22.5	17	19.5	35
CII-C-38-Cit	CPQGLAGQXGIVGLPGCA	cyclic	48	24	19	19	31
CII-C-38-R	CPQGLAGQRGIVGLPGCA	cyclic	45	23.5	25	22	32
CII-C-39-Cit	CIVGLPGQXGERGFPGCA	cyclic	42	22	21.5	20	32
CII-C-39-R	CIVGLPGQRGERGFPGCA	cyclic	38	20	21	20	41
CII-C-3-Cit	CKPGKAGEXGPPGPQGCA	cyclic	36.5	23	24	22	35
CII-C-3-R	CKPGKAGERGPPGPQGCA	cyclic	36	25	21	20.5	37
CII-C-40-Cit	CLPGQRGEXGFPGLPGCA	cyclic	48	27	23	26	38.5
CII-C-40-R	CLPGQRGERGFPGLPGCA	cyclic	51	26	23	23.5	42
CII-C-41-Cit	CAPGASGDXGPPGPVGCA	cyclic	49	20	17	17.5	35.5
CII-C-41-R	CAPGASGDRGPPGPVGCA	cyclic	48	22	17	18	30
CII-C-42-Cit	CGPAGEPGXEGSPGADCA	cyclic	72	24.5	17	19	31.5
CII-C-42-R	CGPAGEPGREGSPGADCA	cyclic	63	20	19	15	34
CII-C-43-cit	CGADGPPGXDGAAGVKCA	cyclic	49.5	25	20.5	20.5	33
CII-C-44-Cit	CAAGVKGDXGETGAVGCA	cyclic	53	24	20.5	18	33
CII-C-44-R	CAAGVKGDRGETGAVGCA	cyclic	74	21	19	17	31
CII-C-45-Cit	CPTGKQGDXGEAGAQGCA	cyclic	48.5	26	20	24	34
CII-C-45-R	CPTGKQGDRGEAGAQGCA	cyclic	43.5	24	19	19	28.5
CII-C-46-Cit	CPSGPAGAXGIQGPQGCA	cyclic	47	2441	22	18	37
CII-C-46-R	CPSGPAGARGIQGPQGCA	cyclic	37	16	16	14	33
CII-C-47-Cit	CIQGPQGPXGDKGEAGCA	cyclic	42	124	19	20	28
CII-C-47-R	CIQGPQGPRGDKGEAGCA	cyclic	38	21.5	26	19	28
CII-C-48-Cit	CEAGEPGEXGLKGHRGCA	cyclic	36	23	17	18.5	31

CII-C-48-R	CEAGEPGERGLKGHRGCA	cyclic	30	18	14	16	25
CII-C-49-Cit	CERGLKGH**XGFTG**LQGCA	cyclic	4145	385	59	19	35.5
CII-C-49-R	CERGLKGH**RGFTG**LQGCA	cyclic	5169	696	22	18	42
CII-C-4-Cit	CPPGPQGAXGFPGTPGCA	cyclic	50	2252	18	21	34
CII-C-4-R	CPPGPQGARGFPGTPGCA	cyclic	321	27	16	16	1238
CII-C-50-cit	CPAGPSGPXGPPGPVGCA	cyclic	39	450	21	19	25
CII-C-50-R	CPAGPSGPRGPPGPVGCA	cyclic	35	17	15.5	15	28
CII-C-51-cit	CPIGPPGPXGRSGETGCA	cyclic	41	176	18	18	29
CII-C-51-R	CPIGPPGPRGRSGETGCA	cyclic	35.5	17	18	16	32
CII-C-52-cit	CGPPGPRGXSGETGPACA	cyclic	84	21	19	20	28
CII-C-52-R	CGPPGPRGRSGETGPACA	cyclic	50	22	22	19	29
CII-C-53-cit	CAFAGLGPXEKGPDPLCA	cyclic	45	20	18.5	18	24
CII-C-53-R	CAFAGLGPREKGPDPLCA	cyclic	49	21	18.5	20	30
CII-C-54-cit	CPDPLQYMXADQAAGGCA	cyclic	62	30	20	19	32.5
CII-C-54-R	CPDPLQYMRADQAAGGCA	cyclic	52	18	17	16	26
CII-C-5-Cit	CLPGVKGHXGYPGLDGCA	cyclic	62	34	17	17	38
CII-C-5-R	CLPGVKGHRGYPGLDGCA	cyclic	47	21	19	16	34
CII-C-6-Cit	CSPGPMGPXGLPGERGCA	cyclic	45	486	17	17	29
CII-C-6-R	CSPGPMGPRGLPGERGCA	cyclic	39	19	20	17	32.5
CII-C-7-Cit	CPRGLPGE**XGRTG**PAGCA	cyclic	4906	343	18	17	1858
CII-C-7-R	CPRGLPGE**RGRTG**PAGCA	cyclic	5980	663	19	17	4963
CII-C-8-Cit	CGLPGE**RGXTG**PAGAACA	cyclic	5985.5	853.5	20	20	868
CII-C-8-R	CGLPGE**RGRTG**PAGAACA	cyclic	3520	291	22	21	1195
CII-C-9-Cit	CPAGAAGAXGNDGQPGCA	cyclic	42	137.5	16	16	28
CII-C-9-R	CPAGAAGARGNDGQPGCA	cyclic	35	20	13	14	30
CII-T-C1-cit-cit	GD**O**GR**O**GE**O**GL**O**GA**XGLTG**X**O**GDA	triple-helical	1641	60	62	23	98
CII-T-C1-cit-R	GD**O**GR**O**GE**O**GL**O**GA**XGLTG**R**O**GDA	triple-helical	408	32	4454	21	120
CII-T-C1-R-R	GD**O**GR**O**GE**O**GL**O**GA**RGLTG**R**O**GDA	triple-helical	752	54	30	352	1136.5
CII-T-C1-R-cit	GD**O**GR**O**GE**O**GL**O**GA**RGLTG**X**O**GDA	triple-helical	5176.5	432	22	90	324
CII-T-D3-cit	GPTGVTGPKGARGAQGP**O**GATGF**O**	triple-helical	63.5	419	25	24	54
CII-T-D3-R	GPTGVTGPKGAXGAQGP**O**GATGF**O**	triple-helical	58	20	21	21	38
CII-T-E10-cit	GAEGP**O**GPQGLAGQXGIVGL**O**GQR	triple-helical	25	20	22	22	25
CII-T-E10-R	GAEGP**O**GPQGLAGQRGIVGL**O**GQR	triple-helical	46	21.5	19.5	20	57.5
CII-T-E17-R	GT**O**GS**O**GPAGASGN**O**GTDGI**O**GAK	triple-helical	28.5	18	15	15	42.5
CII-T-F4-cit-cit	GDKGEAGE**O**GEXGLKGH**XGFTG**LQ	triple-helical	2906	117	19	21.5	26
CII-T-F4-cit-R	GDKGEAGE**O**GEXGLKGH**RGFTG**LQ	triple-helical	3644.5	245	20	18	27
CII-T-F4-R	GDKGEAGE**O**GERGLKGH**RGFTG**LQ	triple-helical	1107	56	22	19	28
CII-T-F4-R-cit	GDKGEAGE**O**GERGLKGH**XGFTG**LQ	triple-helical	1861	78	16	16.5	20
CII-T-J1-cit	GAQGP**O**GLQGM**O**GEXGAAGIAGPK	triple-helical	30.5	4219	24	36	110
CII-T-J1-R	GAQGP**O**GLQGM**O**GERGAAGIAGPK	triple-helical	29.5	1625	19	30	96
CII-T-PC12-R	GASGDRGP**O**GPVGP**O**GLTGPAGE**O**	triple-helical	25	24	24	22	29
CII-T-U1-cit-cit	GDQGV**O**GEAGA**O**GLVGPXGEXGF**O**	triple-helical	23	21	18	18	18
CII-T-U1-cit-R	GDQGV**O**GEAGA**O**GLVGPXGERGF**O**	triple-helical	29	21.5	22	19	21

CII-T-U1-R	GDQGV**O**GEAGA**O**GLVGPRGERGF**O**	triple-helical	24.5	93.5	16	16	19
CII-T-U1-R-cit	GDQGV**O**GEAGA**O**GLVGPRGEXGF**O**	triple-helical	61	1640	23	23	74

Supplementary Table 3: Peptides bound to ACC1Fab in the crystal structures

Listed are the complete sequences of the peptides used for the crystallographic studies, with O = 4-hydroxyproline and X= citrulline, their residue numbers and structure in solution. The recognized epitopes are indicated in italic, with the conserved RG-TG motif emphasized by bold lettering, and the first and last epitope residue numbered in superscript according to their position in the peptide. Peptide residues visible in the electron density map in at least one of the eight copies per asymmetric unit are underlined (CII583-591 is listed twice to indicate the differences in visibility in the two different space groups in which the corresponding structure was determined). In CII616-639, only one of the three peptide chains carry the KKYG extension.

ID (residue nr)	Sequence
C1-CIT365-L(1-18)	GPO ^{4}*GA**RG**L**TG**XOGDA*^{15} GPO-NH_2
C1-CIT365-T(1-33)	$(GPO)_3$GPO ^{13}*GA**RG**L**TG**XOGDA*^{24} $(GPO)_3$
CII583-591/$P2_12_12_1$ (1-30)	$(GPO)_2$GPOGPO ^{13}*GG**RG**L**TG**PI*^{21} GPOGPOGPO
CII583-591/P1 (1-30)	$(GPO)_3$GPO ^{13}*GG**RG**L**TG**PI*^{21} GPO$(GPO)_2$
CII616-639 (1-46/50)	$(GPO)_5$^{16}*GAXGAOGE**RG**E**TG**POGPAGFA*^{36} $(GPO)_3$GKKYG-Biotin